



17

Abstract

18

19 In this study, we introduce a newly-developed upper-air observational instrument for
20 atmospheric research. The “Storm Tracker” (or “NTU mini-Radiosonde”), is an ultra-
21 lightweight (about 20g including battery), multi-channel simultaneous capable radiosonde
22 designed by the Department of Atmospheric Sciences at National Taiwan University.
23 Developed since 2016, the Storm Tracker aims to provide an alternative for observation of
24 atmospheric vertical profiles with a high temporal resolution, especially lower-level
25 atmosphere under severe weather such as extreme thunderstorms and tropical cyclones.

26 Two field experiments were conducted as trial runs in December 2017 and July 2018
27 at Wu-Chi, Taichung, Taiwan, to compare the Storm Tracker with the widely used Vaisala
28 RS41 radiosonde. Among 53 co-launches of the Storm Tracker and Vaisala RS41 radiosondes,
29 the raw measurements of pressure, wind speed, and wind direction are highly consistent
30 between the Storm Tracker and Vaisala RS41. However, a significant daytime warm bias was
31 found due to solar heating. A metal shield specifically for the Storm Tracker was thus installed
32 and shows good mitigation for the warm biases.

33 With the much lower costs of the sondes and the simultaneous multi-channel receiver,
34 the Storm Tracker system has been proved to be beneficial for high-frequency observational
35 needs in atmospheric research.

36



37 **1. Introduction**

38 With a long history of development, the upper-air radiosonde has been one of the
39 essential and the most reliable method to measure the atmosphere above us so far. Operational
40 weather agencies worldwide share their daily to twice-a-day (00UTC and 12UTC) radiosonde
41 observational data through WMO GTS (Global Telecommunication System) for synoptic
42 weather analysis and numerical model forecast. According to the European Centre for Medium-
43 Range Weather Forecasts (ECMWF), in 2017, there are about 818 upper-air radiosonde
44 stations worldwide in addition to more than twelve radiosonde manufactures (Ingleby 2017).
45 So far, most radiosonde manufacturers had participated in the field inter-comparison program
46 hosted by World Meteorological Organization (WMO) throughout 1984–2010, and there were
47 11 different types of operational radiosondes processed in the recent inter-comparison
48 experiment at Yangjiang, China in 2011 (Nash *et al.* 2011)

49 Among all different types of radiosondes, the mostly used Vaisala RS41 radiosonde
50 weighs 110g, and the previous version RS92 weighs 280g. The Japan radiosonde from Meisei
51 Corporation, iMS-100 weighs 38g only, which is so far the lightest operational radiosonde.
52 However, for different purposes in different field campaigns, a large number of radiosondes
53 are often necessary within a short period to acquire much higher temporal resolution data. For
54 the atmospheric research community, most of these radiosondes on the market are often a
55 burden regarding the research budget.

56 In this study, we introduce a newly-developed, smaller, lighter, and cheaper upper-air
57 radiosonde system designed with the capability of simultaneously receiving multiple
58 radiosondes, which is explicitly for high temporal resolution observations on mesoscale
59 weather systems. This so-called Storm Tracker system, developed at the Department of
60 Atmospheric Sciences at National Taiwan University, has been tested in several field
61 experiments since 2016. In section 2, the configuration of the Storm Tracker system is



62 described in detail. Two trial runs of preliminary comparisons between the Storm Tracker and
63 Vaisala RS41 radiosonde are discussed in section 3. Section 4 concludes the current status of
64 the Storm Tracker system and its applications in different field campaigns.

65

66 **2. Configuration for Storm Tracker Upper-air Observation System**

67 The Storm Tracker upper-air observation system consists of the upper-air radiosonde
68 (the Storm Tracker) and the surface signal receiving unit (the Ground Receiver). The overall
69 configuration is described in this section. Figure 1 shows the system block diagram of the
70 Storm Tracker system.

71 **a. The Storm Tracker radiosonde**

72 The Storm Tracker radiosonde is packed with sensors and supporting hardware as
73 shown in Figure 2. The main portion includes the ATMEGA328p microcontroller, the U-blox
74 MAX7-Q GPS sensor, the Bosch BMP280 pressure sensor, the TE-Connectivity HTU21D
75 temperature-humidity sensor, and the LoRa™ transmitter.

76 The central processor of the Storm Tracker is the Microchip ATMEGA328p
77 microcontroller (Atmel Corporation, 2015) with a 2KB of ram and a 32KB of program memory,
78 running at 3.3V with 8MHz clock speed to minimize the power consumption. The
79 microcontroller processes all measurements from the sensors and sends them to the radio
80 transmitter.

81 For the GPS module, the U-blox MAX-7Q is selected (U-Blox, 2014), and the pulse
82 per second output is connected to the MCU for time synchronization. This GPS module
83 provides the geolocation and speed as well as the direction of the Storm Tracker. Also, a chip
84 antenna is chosen to minimize the weight and size, as well as an on-board signal amplifier and



85 a filter to maximize the performance. The overall GPS module possesses an accuracy of 2.0 m
86 for horizontal position and 0.1 m/s for velocity (U-Blox, 2014).

87 The pressure sensor on the Storm Tracker is Bosch BMP280, with an overall operation
88 range from 1100 to 300 hPa and from -40 to 85°C , in addition to a typical accuracy of $\pm 1\text{hPa}$
89 (Bosch Sensortec, 2018). This sensor has been applied to indoor navigation, where a precise
90 pressure measurement is required.

91 For the sensor of temperature (T) and relative humidity (RH), we used the HTU21D, a
92 digital relative humidity sensor with temperature output from the TE Connectivity. This sensor
93 is chosen regarding its high accuracy ($\pm 0.3^{\circ}\text{C}$ in T and $\pm 2\%$ in RH), wide operational range ($-$
94 40 to 125°C , 0 – 100%), the short response time (5 seconds), and cutting-edge energy-saving
95 property (TE Connectivity, 2017). The HTU21D sensor is attached to a 3-cm arm as shown in
96 Figure 2, to extend outside of the protection box to measure the environment. Table 1 briefly
97 summarizes the operational ranges and typical accuracies of atmospheric measurements for
98 Vaisala RS41-SGP radiosonde (VAISALA Corporation, 2017) and the Storm Tracker.

99 The power for Storm Tracker comes from one typical AAA battery with a converter,
100 and this minimizes the total weight. The radio transmitter is powered by LoRa™, which is the
101 long-range, low-power wide-area network technology (Augustin *et al.*, 2016). The radio
102 frequency used by Storm Tracker ranges from 432MHz to 436.5MHz, the configuration for
103 LoRa™ is 7 for spreading factor and 4/5 for code rate with 125kHz channel bandwidth. To
104 extend the battery life, transmit power is set to 18 dB with 1 Hz of transmission frequency.

105 As for the enclosure, we use thick paper with anti-water coating for the Storm Tracker
106 board enclosure. For the external sensors, to mitigate the solar radiation warm bias found
107 during the trial runs in 2017, we design a 1-mm tinplate metal shield to cover the temperature
108 and humidity sensors to prevent direct solar radiation. The whole design of Storm Tracker as
109 shown in Figure 3 is then sent to a local printed circuit board (PCB) assembly factory for



110 production. With the help from the local factory, the final cost of each unit is about 26 US
111 dollars, only about one-tenth of the price of a regular Vaisala RS41 radiosonde.

112 And since the Storm Tracker only weighs about 20g including battery, it can be easily
113 carried by a constant volume foil balloon for constant-height flight, or pilot rubber balloon for
114 regular upper-air observation. Figure 4 shows a typical Storm Tracker launch with a pilot
115 rubber balloon, and Table 2 summarizes the Storm Tracker properties.

116 **b. The Ground Receiver**

117 To receive the radio signal from the Storm Tracker, a micro-computer module is
118 specifically designed to process the data. We use MT7688 SoC (System on Chip) as the core,
119 which runs the OpenWRT operating system at 588MHz with 128MB of ram and 32MB of
120 internal flash (MediaTek, 2016). The SoC connects to an ATMEGA328p (Atmel Corporation,
121 2015) for interfacing with RF (Radio Frequency) modules. Furthermore, a built-in web server
122 uses Node.JS to save and display measured data on the web-page user interface (UI). All data
123 is recorded into an SD memory card and can also be downloaded from the UI. To be portable
124 and easily used in the field, an external USB power supply or DC jack can provide the power
125 for the whole system. Figure 5 shows a complete set of Storm Tracker Ground Receiver
126 installed in a 3D-printed box (9cm*2cm*5cm) with the supporting equipment. The Ground
127 Receiver is finally connected to an omnidirectional antenna with 6dB gain and dual-band (144
128 & 433MHz) frequencies. A typical setup of the Ground Receiver in the field is shown in Figure
129 6.

130 The most powerful feature of the Storm Tracker system based on the design of the
131 Ground Receiver is the ability to receive data from up to 10 radiosondes simultaneously, which
132 provides the opportunity of upper-air observations with extremely high temporal/spatial
133 resolution. In a word, one can launch up to 10 Storm Trackers at once from multiple locations



134 with only one system; or launch a series of Storm Trackers in a short period say an hour, 30
135 minutes, or even 10 minutes depending on the manpower.

136 To accomplish this goal with a single-channel transceiver on the Storm Tracker, time-
137 divided multi-access (TDMA) was implemented into the Storm Tracker system. Since each
138 Storm Tracker only takes about 76ms for data transmission, the system splits every second into
139 10-time slots, and each Storm Tracker transmits the data on the different time slots pre-assigned
140 by the user. Therefore, the Ground Receiver is constantly scanning ten different frequencies
141 per second and tracking up to 10 Storm Trackers at the same time. If the Storm Trackers were
142 in the air at the same time and the data were received simultaneously, each Storm Tracker still
143 takes up the different frequencies from 432 to 436.5 MHz to prevent any interference.

144 A newer version of the Ground Receiver is currently underway, which is powered by
145 Raspberry Pi SBC (Single Board Computer) and a unique in-house designed LoRa™ gateway,
146 which can receive 8-channel simultaneously. In the future, this new design with TDMA could
147 monitor 80 Storm Trackers at the same time.

148

149 **3. The intercomparison between the Storm Tracker and Vaisala RS41-SGP**

150 Two trial field experiments were conducted to examine the actual performance of the
151 Storm Tracker system. In these trial runs, the Storm Tracker was launched attaching to a
152 Vaisala RS41-SGP radiosonde for intercomparison of the measurements as shown in Figure 7.
153 The first trial run was conducted for four days in December 2017 at Wu-Chi, Taichung, Taiwan,
154 and in total 28 flights of Storm Tracker and Vaisala RS41 were launched.

155 The raw data from both radiosondes were processed and linearly interpolated according
156 to the same heights, which then separated into daytime (8 ~ 18LST) and nighttime (18 ~ 8 LST).
157 Since the radiosondes were only launched when the sky is clear without clouds, the average



158 vertical profile from the Vaisala RS41 shows a clear signature of subsidence and an overall dry
159 atmosphere (Figure 8).

160 The results of the intercomparison are shown in Figure 9. According to the temperature
161 difference in Figure 9, the temperature sensor had experienced significant solar heating during
162 the daytime, which also caused the solar radiation dry bias. During the daytime, the mean warm
163 bias is 5.68°C, and the dry bias is 6.42%. Nevertheless, during the nighttime, both temperature
164 and humidity show good agreements between the Storm Tracker and Vaisala RS41, with the
165 mean differences of 0.35°C and 1.75%. The vertical profiles of the differences during daytime
166 and nighttime are shown in Figure 10, which also shows the apparent heating and drying over
167 the whole atmosphere during the daytime.

168 On the other hand, in Figure 9 the differences in measurements such as the pressure and
169 winds are not mainly affected by solar heating, which shows a relatively good agreement
170 between the Storm Tracker and Vaisala RS41. The mean difference for the measurements of
171 pressure is 1.69hPa (0.75hPa) below 0°C (above 0°C), which lies within the error of the sensor
172 according to Table 1. And since the GPS systems in both the Storm Tracker and Vaisala RS41
173 track almost the same satellites, the mean errors for wind measurements are insignificant with
174 that of wind speed of 0.09m/s, and -0.15 degrees for wind direction.

175 Since the results from the trial run in 2017 show that the solar radiation is an important
176 factor affecting the temperature and moisture measurements, we installed a thin metal shell (i.e.
177 the “hat”) around the temperature/humidity sensor as shown in Figure 3 to prevent the direct
178 solar heating in the second trial run conducted in July 2018. In the second run, every launch
179 includes a Vaisala RS41 attached with two Storm Trackers, one is with the hat and one is not.
180 Similar to the first run, in the second run, the data from 19 co-launches under the clear sky
181 were collected. As shown in Figure 11, the average vertical profile shows an overall dry



182 atmosphere with slight subsidence above 850hPa. The maximum height of the measurements
183 is lower in the second run than that in the first run due to the different batteries used in 2018.

184 Figure 12 shows the histograms for the comparison between the Storm Tracker w/wo
185 the hat. The results of the pressure and winds measurements show almost no difference between
186 the Storm Trackers w/wo the hat, however, during the daytime the mean temperature warm
187 bias drops from 2.47°C to 2.18°C by adding the hat. The standard deviation also drops from
188 1.2°C to 0.86°C. Likewise, the mean dry bias for humidity drops from 2.37% drier to 1.27%
189 drier with the hat, which is within the sensor accuracy range as shown in Table 1. And the
190 standard deviation decreases from 4.74% to 4.08%. These results show that the reflective metal
191 shield does help to prevent direct solar heating when the Storm Tracker is in the air.

192 However, the installation of the metal shield causes a further warm bias when there is
193 no solar heating. During the nighttime, even the biases lie within the accuracy range of the
194 sensor, the mean warm bias increases from 0.13°C without the hat to 1.17°C with the hat, and
195 the standard deviation increases from 0.36°C to 0.54°C. The mean humidity bias, on the other
196 hand, drops from 6.11% for Storm Tracker without the hat to 2.11% Storm Tracker with the
197 hat, but the standard deviation slightly increases from 2.67% to 2.87%. During the nighttime,
198 the results show that the metal shield further induces a warm bias, which may be the main cause
199 of the dry bias in the moisture measurement.

200 On average, even though the mean warm bias increases from 1.24°C to 1.66°C if the hat
201 is added, the standard deviation decreases from 1.45°C to 0.87°C. Moreover, the mean humidity
202 bias improves from 2.10% to 0.50% with the hat, and the standard deviation also drops from
203 5.69% to 3.88% with the hat. It is shown that the metal shield installation does prevent the solar
204 radiation heating effects during the daytime even it also introduces an additional warming
205 effect during the night.



206 These results can also be seen in the vertical profiles according to Figure 13. As shown
207 in Figure 13, overall the variances of measurements are lowered by adding the metal shield
208 onto the temperature/humidity sensor. Moreover, Table 3 lists all the statistics for the second
209 intercomparison run between the Storm Tracker w/wo the hat and Vaisala RS41. Even though
210 the metal shield causes a slight warm bias during the nighttime, it mitigates the solar radiation
211 heating effects and the solar radiation dry bias during the daytime when most of the mesoscale
212 convective rainfall occurs. For such events in Taiwan, it is worthwhile to apply these new
213 instruments to acquire much higher resolution data especially for afternoon thunderstorms
214 triggered by daytime solar heating.

215

216 **4. Applications in the field campaigns and the concluding remarks**

217 In 2018, during the Taipei Summer Storm Experiment (TASSE), hourly launches (8
218 ~16LST) of Storm Trackers were conducted among several sites in the Taipei Basin. These
219 data were used to study the urban atmospheric boundary layer variation and the prevailing
220 environment of thunderstorm convection in the afternoon. Figure 14 shows the Storm Tracker
221 paths launched from June 27 to July 3, 2018, during the TASSE. This campaign is a good
222 example to use the Storm Tracker for vertical profiles with high temporal resolution up to every
223 hour at multiple launch sites. The Storm Tracker is a good alternative with a much lower cost
224 and capability for multiple simultaneous observations.

225 Another campaign during typhoon Talim on September 13, 2017, was conducted with
226 two Storm Trackers to see if the observations inside the tropical cyclones are possible. Figure
227 15 shows the flight path and the altitude of the Storm Tracker which uses the larger CR123
228 battery to extend the lifetime. The flight path shows that the Storm Trackers can be carried and
229 observe at a constant altitude and following the outlying wind direction of the typhoon.



230 Although the signal was lost eventually, this launch shows the potential of Storm Tracker to
231 conduct drift sound experiments in the future, and even for more kinds of observational needs.

232 Although the Storm Tracker system is incorporated with the new low-cost sensors, we
233 show that it can accomplish decent performance compared with Vaisala RS41 radiosonde with
234 a significant cost reduction. Moreover, with the capability of tracking multi-tracker
235 simultaneously and incorporating LoRa™ technology, it enables future missions to deploy a
236 large number of radiosondes to collect higher temporal/spatial resolution data.

237 These trial runs show that the Storm Tracker radiosondes still have issues regarding
238 temperature and moisture measurements, but the current configuration with a thin metal shield
239 does help with the daytime biases. More experiments to compare the measurements between
240 the Storm Tracker and Vaisala RS41 are underway, in addition to the intercomparison among
241 different individual instruments such as radiometer. More importantly, with more
242 intercomparison data, the objective correction algorithms are currently developed and tested
243 for better data quality control.

244

245 **Data availability**

246 All field measurement data from our Storm Tracker and Vaisala RS-41-SGP could be accessed
247 through FTP by request.

248 **Authors contribution**

249 Mr. Hwang makes the PCB, program coding and document draft. Dr. Lin supports all funding
250 of this study and coordinated field tests. Dr. Yu joins the discussion of data intercomparison.

251 **Competing interests**

252 The authors declare that they have no conflict of interest.

253



254 **Acknowledgments**

255 The authors would like to thank the RS-41 data sharing from RCEC (Research Center for
256 Environmental Change) in Academic Sinica, and the field test supported by TASSE program
257 (MOST 108-2119-M-002-022) which is managed by Prof. Hung-Chi Kuo, National Taiwan
258 University. We also appreciate the efforts of the associate editor and the anonymous reviews
259 whose comments to improve this paper.

260 **References**

- 261 Atmel Corporation : ATmega328P 8-bit AVR Microcontroller with 32K Bytes In-System
262 Programmable Flash Datasheet. ATmega328P [DATASHEET] 7810D–AVR–01/15,
263 294 pp, [http://ww1.microchip.com/downloads/en/DeviceDoc/Atmel-7810-
264 Automotive-Microcontrollers-ATmega328P_Datasheet.pdf](http://ww1.microchip.com/downloads/en/DeviceDoc/Atmel-7810-Automotive-Microcontrollers-ATmega328P_Datasheet.pdf). 2015
- 265 Augustin, A., Yi, J., Clausen, T., Townsley, W.M.: A Study of LoRa: Long Range & Low
266 Power Networks for the Internet of Things. *Sensors*, 16, 1466.
267 <https://doi.org/10.3390/s16091466>. 2016
- 268 Bosch Sensortec: Data sheet BMP280 Digital Pressure Sensor. BST-BMP280-DX001-19, 49
269 pp, [https://ae-bst.resource.bosch.com/media/_tech/media/datasheets/BST-BMP280-
270 DS001.pdf](https://ae-bst.resource.bosch.com/media/_tech/media/datasheets/BST-BMP280-DS001.pdf). 2018
- 271 Ingleby, B. : An assessment of different radiosonde types 2015/2016. ECMWF Technical
272 Memoranda, 807. Pp77. 2017
- 273 MediaTek: MediaTek MT7688 Datasheet, 294 pp,
274 <http://labs.mediatek.com/en/chipset/MT7688>. 2016
- 275 Nash, J., Oakley, T., Vömel, H., Wei, L.: WMO intercomparison of high quality radiosonde
276 systems, Yangjiang, China, 12 July–3 August 2010. World Meteorological
277 Organization, Instruments and Observing methods, report No, 107. 2011



- 278 TE Connectivity : HTU21D(F) RH/T SENSOR IC Digital Relative Humidity sensor with
279 Temperature output. HTU21D(F) RH/T SENSOR IC, 22pp,
280 [https://www.te.com/commerce/DocumentDelivery/DDEController?Action=showdoc](https://www.te.com/commerce/DocumentDelivery/DDEController?Action=showdoc&DocId=Data+Sheet%7FHPC199_6%7FA6%7Fpdf%7FEnglish%7FENG_DS_HPC199_6_A6.pdf%7FCAT-HSC0004)
281 [&DocId=Data+Sheet%7FHPC199_6%7FA6%7Fpdf%7FEnglish%7FENG_DS_HPC](https://www.te.com/commerce/DocumentDelivery/DDEController?Action=showdoc&DocId=Data+Sheet%7FHPC199_6%7FA6%7Fpdf%7FEnglish%7FENG_DS_HPC199_6_A6.pdf%7FCAT-HSC0004)
282 [199_6_A6.pdf%7FCAT-HSC0004](https://www.te.com/commerce/DocumentDelivery/DDEController?Action=showdoc&DocId=Data+Sheet%7FHPC199_6%7FA6%7Fpdf%7FEnglish%7FENG_DS_HPC199_6_A6.pdf%7FCAT-HSC0004). 2017
- 283 U-Blox : MAX-7 u-blox 7 GNSS modules Data Sheet. UBX-13004068, 24 pp,
284 [https://www.u-blox.com/sites/default/files/products/documents/MAX-](https://www.u-blox.com/sites/default/files/products/documents/MAX-7_DataSheet_%28UBX-13004068%29.pdf)
285 [7_DataSheet_%28UBX-13004068%29.pdf](https://www.u-blox.com/sites/default/files/products/documents/MAX-7_DataSheet_%28UBX-13004068%29.pdf). 2014
- 286 VAISALA Corporation : Vaisala Radiosonde RS41-SGP. B211444EN-E, 2pp,
287 [https://www.vaisala.com/sites/default/files/documents/WEA-MET-RS41SGP-](https://www.vaisala.com/sites/default/files/documents/WEA-MET-RS41SGP-Datasheet-B211444EN.pdf)
288 [Datasheet-B211444EN.pdf](https://www.vaisala.com/sites/default/files/documents/WEA-MET-RS41SGP-Datasheet-B211444EN.pdf). 2017
289



290 **Caption List**

291

292 Table 1. List of the operational ranges and typical accuracies of basic atmospheric
293 measurements for Vaisala RS41-SGP radiosonde (VAISALA Corporation 2017) and the Storm
294 Tracker.

295

296 Table 2. Characteristics of Storm Tracker.

297

298 Table 3. Temperature and Humidity Error (Storm Tracker – Vaisala RS41-SGP) Statistics for
299 the second intercomparison experiment in July 2018 at Wu-Chi.

300

301 Figure 1. System block diagram for the Storm Tracker system, including Storm Tracker (left)
302 and Receiver (right). The part number for the chipset is indicated in the box, and the arrow
303 indicated the dataflow.

304

305 Figure 2. Photo of a PCB assembled Storm Tracker product from the PCBA, in addition to a
306 reference (ruler in centimeters) and a AAA battery. The diameter of the Storm Tracker is
307 58.1mm x 50.2mm (height x width, including sensor arm). The GPS antenna and GPS module
308 are located on the top right of Storm Tracker, along with the power switching on the top left.
309 The RF module is located on the bottom, and the red wire is the quarter-wave antenna. The
310 extended arm hosts the temperature and humidity sensor, and the pins on the bottom are for
311 programming and debug purposes. Lastly, in the middle are the microcontroller and pressure
312 sensor.

313



314 Figure 3. A Storm Tracker with the enclosure and the metal shield. The enclosure is composed
315 of paper, and the hole on the top (bottom) is for connecting to the balloon (passing of the
316 antenna). The metal shield is attached to the PCB board with hot glue.

317

318 Figure 4. A Storm Tracker (without enclosure) launched with a pilot rubber balloon during a
319 field campaign.

320

321 Figure 5. Photo of a Storm Tracker Ground Receiver. On the right are the GPS module and RF
322 module to receive the signal, along with the USB and DC power jack for power input and the
323 console access. In the middle is the central processor, which handles data recording and hosts
324 the website. On the left is the SD card for storage. On the top are the indicator LEDs, which
325 show the current status of the receiver and the received data channels.

326

327 Figure 6. A typical setup of the ground receiver in the field, with the 433Mhz antenna in the
328 middle, and the receiver, GPS antenna and power bank at the bottom black box.

329

330 Figure 7. A photo of the intercomparison launch setup. The Storm Tracker is attached to the
331 side of a Vaisala RS41 radiosonde with double side tape.

332

333 Figure 8. The skew-T-log-P diagram of the average vertical profile measured by Vaisala RS41
334 radiosondes during the intercomparison run in December 2017 at Wu-Chi. The thick red line
335 indicated the dew point and the thick blue line indicated the temperature profile.

336

337 Figure 9. Histograms of the differences between the Vaisala RS41 radiosonde and the Storm
338 Tracker separated by daytime and nighttime during the first intercomparison run in 2017 at Wu



339 Chi. The blue histograms show the data during the nighttime, and the red histograms show the
340 data during the daytime.

341

342 Figure 10. The vertical profiles for temperature and humidity differences during both the
343 daytime and nighttime in the first intercomparison run. The lines indicated the mean, and the
344 one standard deviation ranges are shaded. The red color indicates daytime data, and blue color
345 indicates nighttime data.

346

347 Figure 11. Similar to Figure 8 except for the second intercomparison run in July 2018 at Wu-
348 Chi.

349

350 Figure 12. Similar to Figure 9 except for the differences between the both configurations and
351 the Vaisala RS41 radiosondes during the second intercomparison run. The blue histograms
352 show the data for Storm Tracker with the hat, and the red histograms show the data for Strom
353 Tracker w/o the hat.

354

355 Figure 13. Similar to Figure 10 except for the differences between the Storm Trackers with and
356 without the metal shield.

357

358 Figure 14. Picture of the tracks of the Storm Trackers launched during 27 Jun–3 Jul, 2018 in
359 the TASSE-2018 field campaign. The launching sites include Chidu, Banqiao and Shezi. Credit
360 to Google Earth Pro for providing the satellite image.

361

362 Figure 15. Three balloon tracks during Typhoon Talim (top) and the height profile of the Strom
363 Tracker 0 (bottom). The launching site is located on campus of the National Taiwan University.



364 The maximum range of the Storm Tracker from the site is 132km, in which the Storm Tracker
365 could maintain at about 6200m height. Credit to Google Earth Pro for providing the satellite
366 image.
367



368 **Tables**

369

370 **Table 1. List of the operational ranges and typical accuracies of basic atmospheric**
 371 **measurements for Vaisala RS41-SGP radiosonde (VAISALA Corporation 2017) and the**
 372 **Storm Tracker.**

373

Spec	Vaisala RS41-SGP	Storm Tracker
P Range	sfc. - 3 hPa	1100 - 300 hPa
P Accu.	1.0 hPa (>100 hPa)	1 hPa (0 - 65 °C)
		1.7 hPa (-20 - 0 °C)
T Range	-90 - +60 °C	-40 - +125 °C
T Accu.	0.3 °C (<16 km)	0.3 °C
	0.4 °C (>16 km)	
RH Range	0 - 100 %	0 - 100 %
RH Accu.	4%	2%
Horizontal WIND SPEED		
Accu.	0.15 m/s	0.1 m/s
		(Hor. Accu.: 2.5 m)

374

375



376 **Table 2. Characteristics of Storm Tracker.**

377

Characteristic	Storm Tracker
Sensors	Temperature, Humidity, Pressure, GPS location, Wind Speed
Frequency	432 MHz to 436.5 MHz
Channels	Ten simultaneous Channels
Time Resolution	1s (1Hz)
Power	1x AAA Battery
Battery Life	2 - 4 Hours
Weight	20g with 1x AAA Battery
Dimension	58.1 mm x 50.2mm x 30mm

378

379



380 **Table 3. Temperature and Humidity Error (Storm Tracker – Vaisala RS41-SGP)**

381 **Statistics for the second intercomparison experiment in July 2018 at Wu-Chi.**

	Temperature Error (°C)		Humidity Error (%)	
	W/o Hat	With Hat	W/o Hat	With Hat
Night Time	0.13±0.36	1.17±0.54	6.11±2.67	2.11±2.87
Day Time	2.47±1.20	2.18±0.86	-2.37±4.74	-1.27±4.08
Total	1.24±1.45	1.66±0.87	2.10±5.69	0.50±3.88

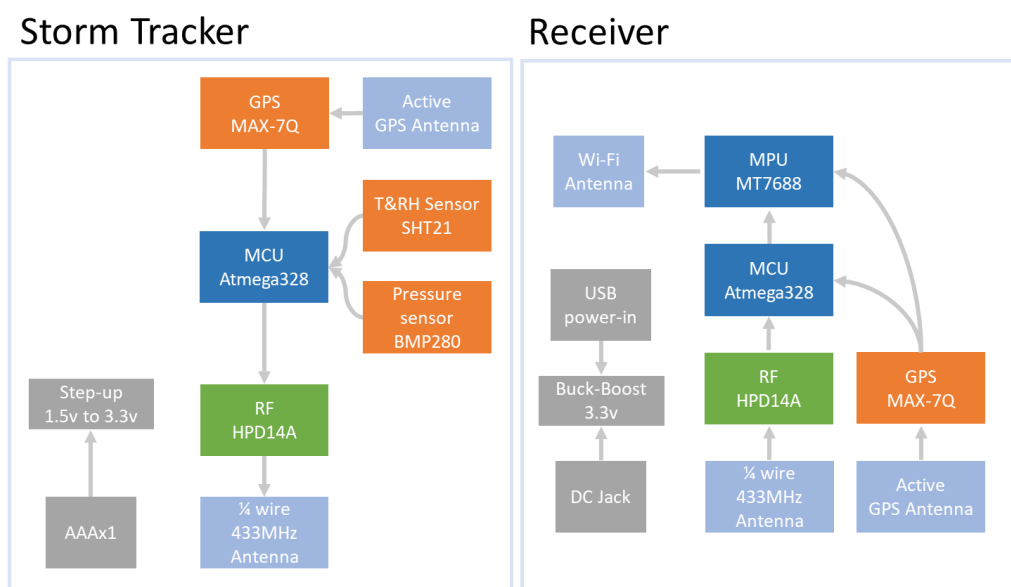
382

383



384 **Figures**

385



386

387

388 **Figure 1. System block diagram for the Storm Tracker system, including Storm Tracker**

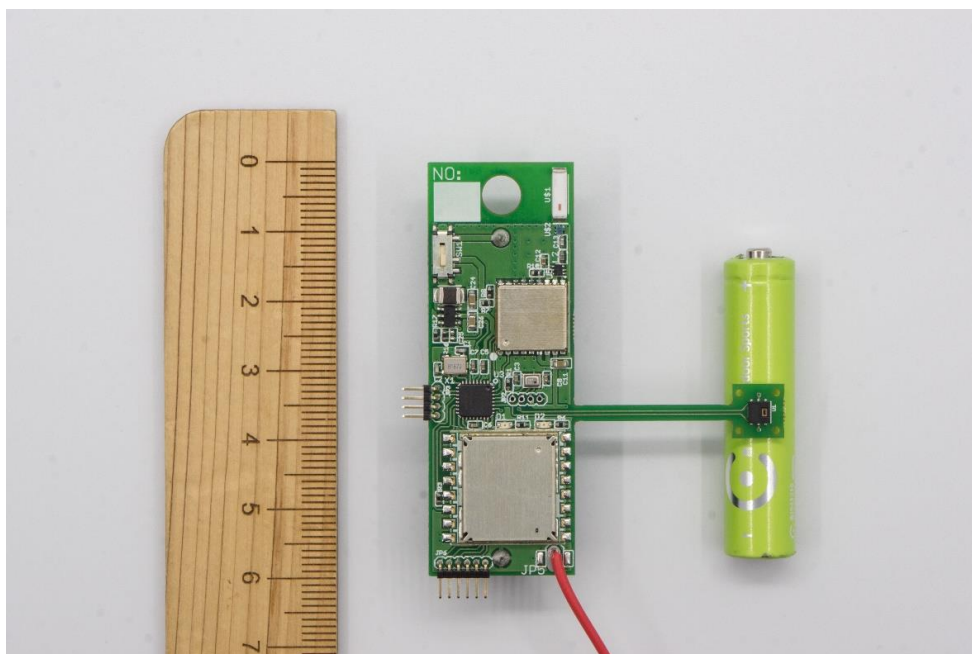
389 **(left) and Receiver (right). The part number for the chipset is indicated in the box, and**

390 **the arrow indicated the dataflow.**

391



392



393

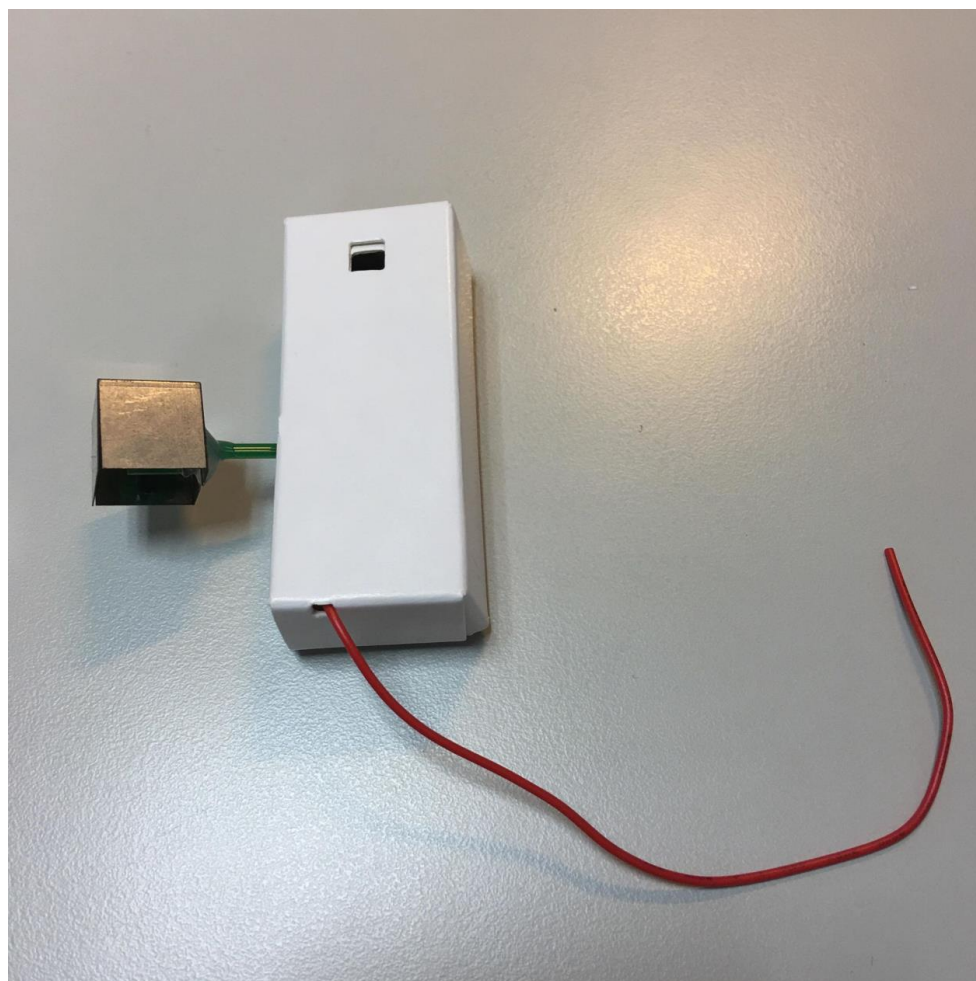
394

395 **Figure 2. Photo of a PCB assembled Storm Tracker product from the PCBA, in addition**
396 **to a reference (ruler in centimeters) and a AAA battery. The diameter of the Storm**
397 **Tracker is 58.1mm x 50.2mm (height x width, including sensor arm). The GPS antenna**
398 **and GPS module are located on the top right of Storm Tracker, along with the power**
399 **switching on the top left. The RF module is located on the bottom, and the red wire is the**
400 **quarter-wave antenna. The extended arm hosts the temperature and humidity sensor,**
401 **and the pins on the bottom are for programming and debug purposes. Lastly, in the**
402 **middle are the microcontroller and pressure sensor.**

403



404



405

406

407 **Figure 3. A Storm Tracker with the enclosure and the metal shield. The enclosure is**
408 **composed of paper, and the hole on the top (bottom) is for connecting to the balloon**
409 **(passing of the antenna). The metal shield is attached to the PCB board with hot glue.**

410



411



412

413

414 **Figure 4. A Storm Tracker (without enclosure) launched with a pilot rubber balloon**

415 **during a field campaign.**

416



417



418

419

420 **Figure 5. Photo of a Storm Tracker Ground Receiver. On the right are the GPS module**
421 **and RF module to receive the signal, along with the USB and DC power jack for power**
422 **input and the console access. In the middle is the central processor, which handles data**
423 **recording and hosts the website. On the left is the SD card for storage. On the top are the**
424 **indicator LEDs, which show the current status of the receiver and the received data**
425 **channels.**

426



427



428

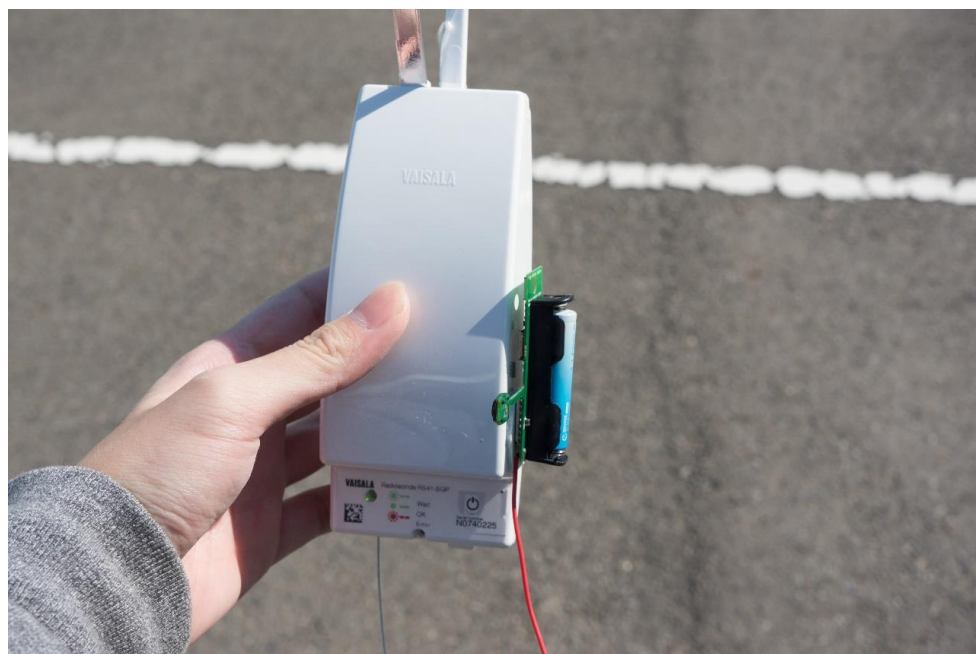
429

430 **Figure 6. A typical setup of the ground receiver in the field, with the 433Mhz antenna in**
431 **the middle, and the receiver, GPS antenna and power bank at the bottom black box.**

432



433



434

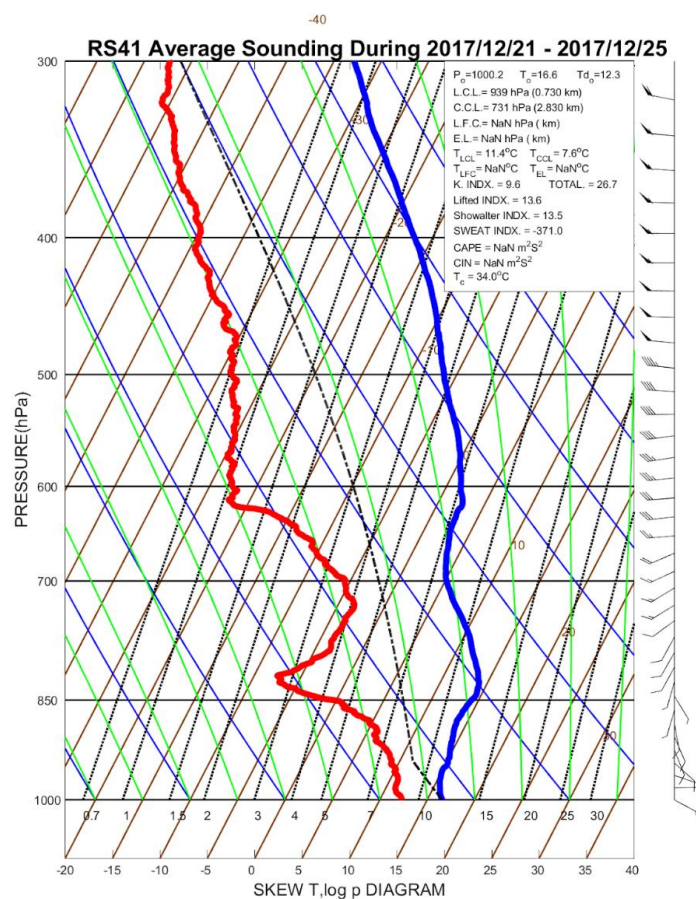
435

436 **Figure 7. A photo of the intercomparison launch setup. The Strom Tracker is attached to**
437 **the side of a Vaisala RS41 radiosonde with double side tape.**

438



439



440

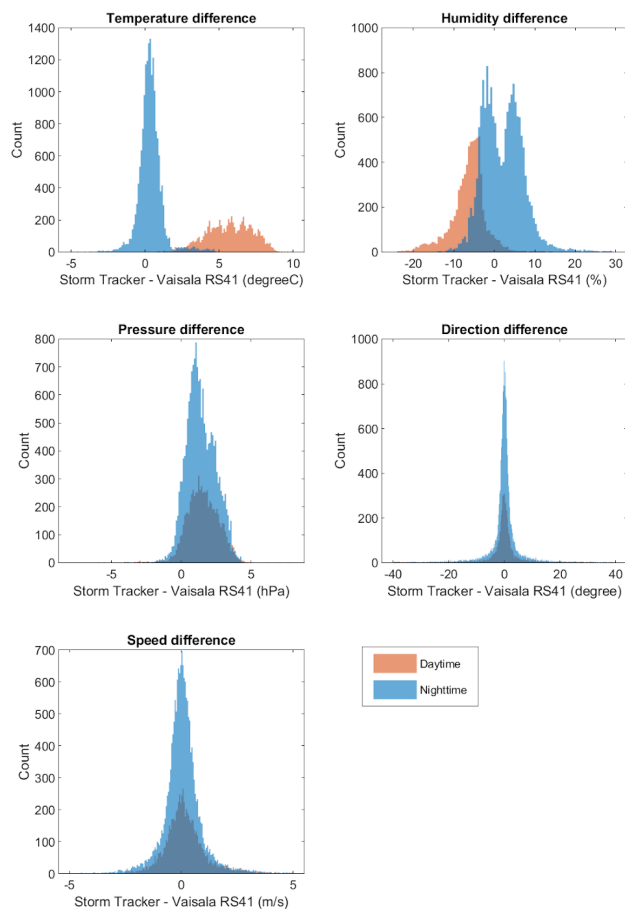
441

442 **Figure 8. The skew-T-log-P diagram of the average vertical profile measured by Vaisala**
443 **RS41 radiosondes during the intercomparison run in December 2017 at Wu-Chi. The**
444 **thick red line indicated the dew point and the thick blue line indicated the temperature**
445 **profile.**

446



447



448

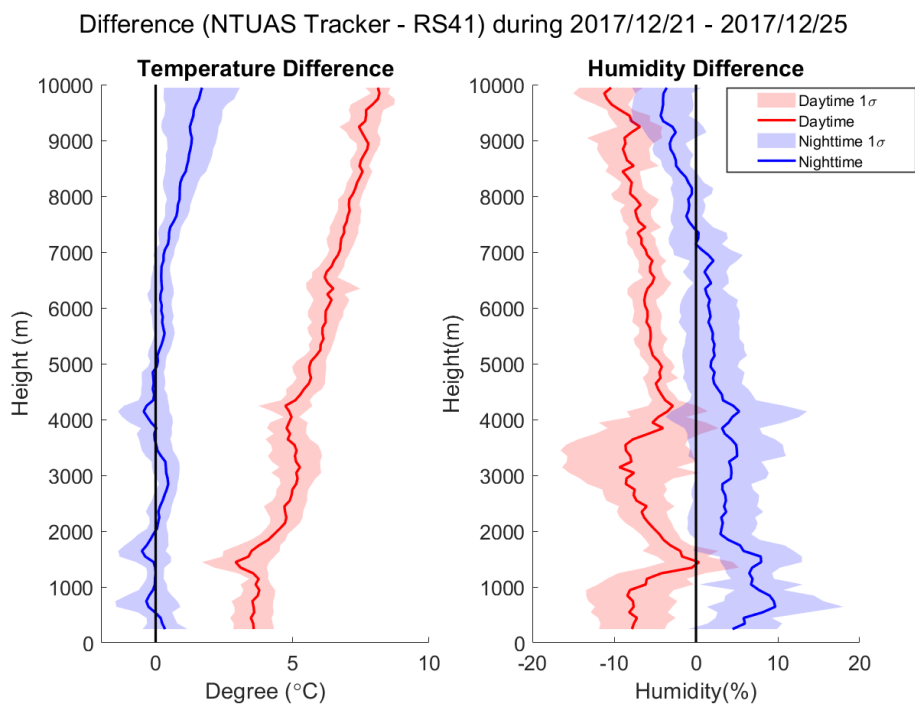
449

450 **Figure 9. Histograms of the differences between the Vaisala RS41 radiosonde and the**
451 **Storm Tracker separated by daytime and nighttime during the first intercomparison run**
452 **in 2017 at Wu Chi. The blue histograms show the data during the nighttime, and the red**
453 **histograms show the data during the daytime.**

454



455



456

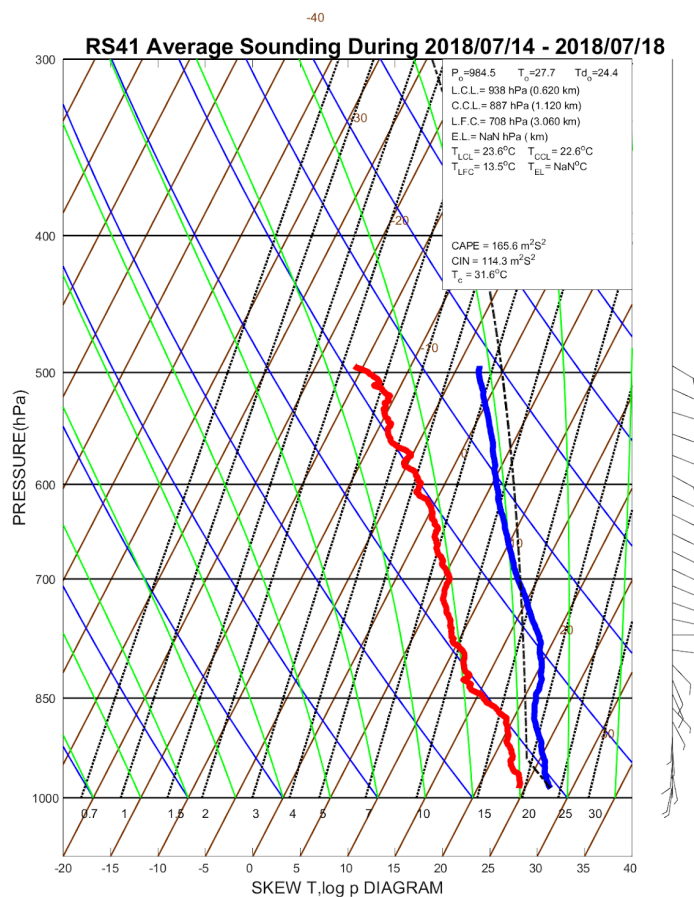
457

458 **Figure 10. The vertical profiles for temperature and humidity differences during both the**
459 **daytime and nighttime in the first intercomparison run. The lines indicated the mean,**
460 **and the one standard deviation ranges are shaded. The red color indicates daytime data,**
461 **and blue color indicates nighttime data.**

462



463



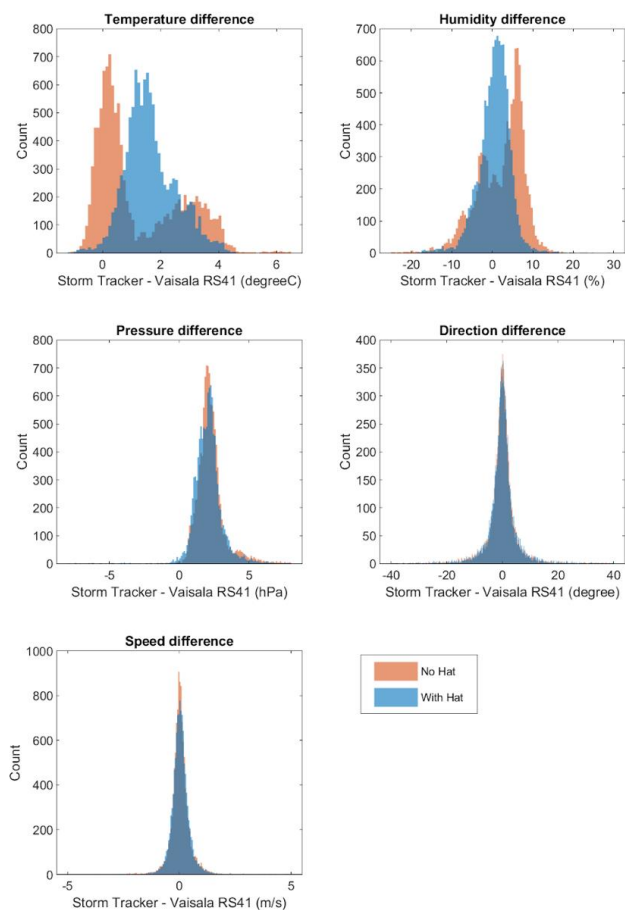
464

465

466 **Figure 11. Similar to Figure 8 except for the second intercomparison run in July 2018 at**

467 **Wu-Chi.**

468



469

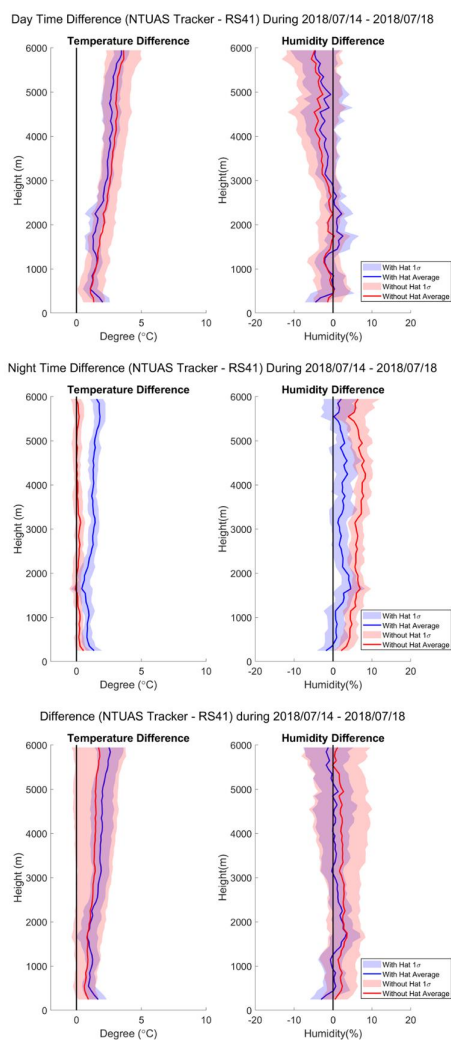
470

471 **Figure 12. Similar to Figure 9 except for the differences between the both configurations**
472 **and the Vaisala RS41 radiosondes during the second intercomparison run. The blue**
473 **histograms show the data for Storm Tracker with the hat, and the red histograms show**
474 **the data for Storm Tracker w/o the hat.**

475



476



477

478

479 **Figure 13. Similar to Figure 10 except for the differences between the Storm Trackers**
480 **with and without the metal shield.**

481



482



483

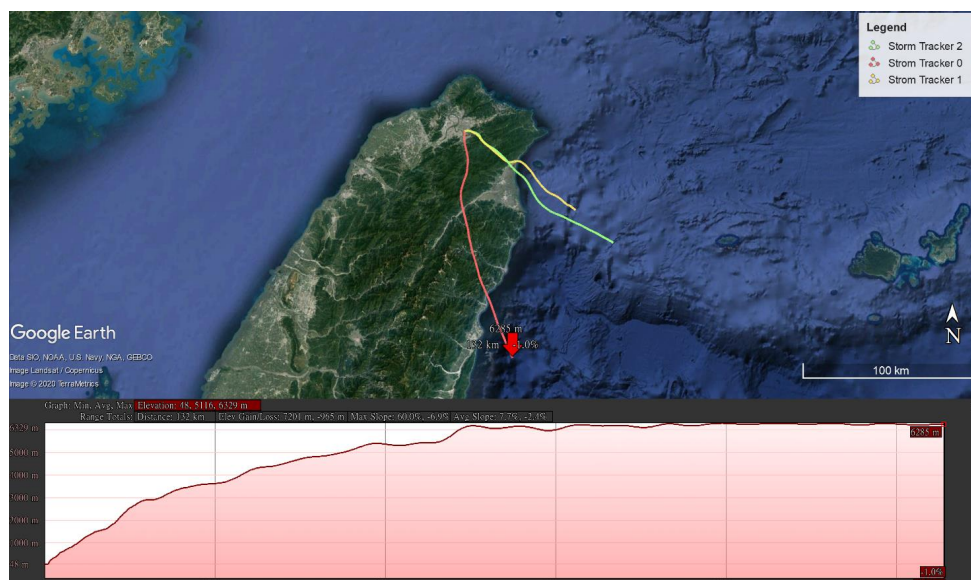
484

485 **Figure 14. Picture of the tracks of the Storm Trackers launched during 27 Jun–3 Jul,**
486 **2018 in the TASSE-2018 field campaign. The launching sites include Chidu, Banqiao and**
487 **Shezi. Credit to © Google Earth Pro for providing the satellite image.**

488



489



490

491

492 **Figure 15. Three balloon tracks during Typhoon Talim (top) and the height profile of the**
493 **Storm Tracker 0 (bottom). The launching site is located on campus of the National**
494 **Taiwan University. The maximum range of the Storm Tracker from the site is 132km, in**
495 **which the Storm Tracker could maintain at about 6200m height. Credit to © Google Earth**
496 **Pro for providing the satellite image.**

497